Numerical Simulation of the Laminar Forced Convective Heat Transfer between Two Concentric Cylinders

Ioan Sarbu * and Anton Iosif

Department of Building Services Engineering, Polytechnic University of Timisoara, Piata Victoriei, no 2A, 300006 Timisoara, Romania; anton.iosif@upt.ro

* Correspondence: ioan.sarbu@upt.ro; Tel.: +40-256-403-991

Abstract: The dual reciprocity method (DRM) is a highly efficient numerical method of transforming domain integrals arising from the non-homogeneous term of the Poisson equation into equivalent boundary integrals. In this paper, the velocity and temperature fields of laminar forced heat convection in a concentric annular tube, with constant heat flux boundary conditions, have been studied using numerical simulations. The DRM has been used to solve the governing equation, which is expressed in the form of a Poisson equation. A test problem is employed to verify the DRM solutions with different boundary element discretizations and numbers of internal points. The results of the numerical simulations are discussed and compared with exact analytical solutions. Good agreement between the numerical results and exact solutions is evident, as the maximum relative errors are less than 5% to 6%, and the R^2-values are greater than 0.999 in all cases. These results confirm the effectiveness and accuracy of the proposed numerical model, which is based on the DRM.

Keywords: concentric annular tube; laminar flow; heat convection; heat flux; boundary condition; dual reciprocity method; numerical model

1. Introduction

Modern computational techniques facilitate solving problems with imposed boundary conditions using different numerical methods [1–9]. The numerical analysis of heat transfer [10–14] has been independently, though not exclusively, developed in four main streams: the finite difference method (FDM) [15,16], the finite volume method (FVM) [17], the finite element method (FEM) [18–20], and the boundary element method (BEM) [21–23]. The FDM is based on using Taylor series expansion to find approximation formulas for derivative operators. The basic concept of the FVM is derived from physical conservation laws applied to control volumes. The FDM, FVM and FEM depend on the mesh that discretizes the domain via a special scheme. The FEM and BEM are based on the integral equation for heat conduction. This equation can be obtained from the differential equation using the variational calculus.

The BEM uses a fundamental solution to convert a partial differential equation to an integral equation. In the BEM, only the boundary is discretized and an internal point's position can be freely defined. This method has the immediate advantage of reducing the dimensionality of the problem by one. Additionally, the BEM naturally handles the problems caused by dynamic geometry. Unlike the FEM, which requires that the domain be meshed, the BEM only discretizes the boundary. Therefore, the amount of data necessary for solving a problem can be greatly reduced [21–24]. A complete review of the BEM's domain integrals is presented in [25].

The BEM, an effective and promising numerical analysis tool due to its semi-analytical nature and ability to reduce a problem's dimension, has been successfully applied to the homogeneous linear heat conduction problem [26]. In the context of BEM-based velocity-vorticity formulation, the work of Žagar and Škerget [27] was one of the first attempts to solve 3D viscous laminar flow by BEM. The BEM has also been used to solve direct and inverse heat conduction problems [22,28,29]. However, its extension to non-homogeneous and non-linear problems is not straightforward. Therefore, applications of the BEM to heat convection problems have not been sufficiently studied, and are still in the development stage. Because the effects of convection are of considerable importance in many heat transfer phenomena, more research should focus on these effects. However, applying the BEM to such problems has drawbacks—the required fundamental solution depends on the thermal conductivity, and it is difficult to model heat generation rates (due to heat sources), because they introduce domain integrals [30].

Several researchers have also worked on a combination of boundary element and finite element methods. A combined BEM-FEM model for the velocity-vorticity formulation of the Navier-Stokes equations was developed by Žunič et al. [31] to solve 3D laminar fluid flow. In the field of viscous fluid flow numerical simulation, an important work was done by Young et al. [32] using primitive variable formulation of Navier-Stokes equations. They computed pressure fields with BEM and momentum equation with a three-steps FEM. In the field of viscous fluid flow numerical simulation with velocity-vorticity formulation of Navier-Stokes equations, contributions were made by Young et al. [33]. In their work, BEM was used to obtain boundary velocities and normal velocity fluxes implicitly, and then explicitly the internal velocities and boundary vorticities were computed by derivation of kinematical integral equations. Simulations, as well as experiments, of turbulent flow have also been extensively investigated [34]. Hsieh and Lien [35] considered numerical modelling of buoyancy-driven turbulent flows in enclosures, using the Reynolds-average Navier-Stokes approach.

Recently, the radial integration method (RIM) has been developed by Gao [36], which did not require fundamental solutions to basis functions, and can remove various singularities appearing in domain integrals. However, although the radial integration BEM is very flexible in treating the general non-linear and non-homogeneous problems, the numerical evaluation of the radial integrals is very time-consuming compared to other methods [37–39], especially for large 3D problems.

To approximate a solution to the heat conduction equation using boundary integrals, the dual reciprocity method (DRM), introduced by Nardini and Brebbia [40], can be used. The DRM preserves the advantages of the BEM: a shorter computational time than the FEM, and a reduced number of boundary elements. Since its introduction, the DRM has been applied to engineering problems in many fields [41–43]. In the DRM, an available fundamental solution is used for the complete governing equation, and the domain integral arising from the heat source-like term is transferred to the boundary using radial interpolation functions [44–46].

In this paper, the velocity and temperature fields of laminar forced heat convection in a concentric annular tube with constant heat flux on the boundaries were studied using numerical simulations. The DRM was used to solve the governing equation, which is expressed mathematically in the form of a Poisson equation. A test problem was employed to verify the DRM solutions with different boundary element discretizations and different numbers of internal points, and the results of the numerical simulations are discussed and compared with exact analytical solutions to determine their convergence and accuracy. A concentric annular tube was chosen because of its simplicity and ability to provide an exact solution, allowing the basic nature of the proposed model for convection problems to be analysed in detail [47,48]. Therefore, present research efforts aiming at the establishment of the DRM's applicability to heat convection are confirmed, and could eventually be extended to the study of other heat transfer systems.

2. Physical Problem and Its Mathematical Formulation

Consider an incompressible Newtonian fluid of density ρ, thermal conductivity λ, and specific heat c contained between two stationary concentric cylinders (i.e., in a concentric annular tube). The inner and outer cylinders have radii of R_i and R_o, respectively. Figure 1 shows a schematic of the annular tube and co-ordinate system.
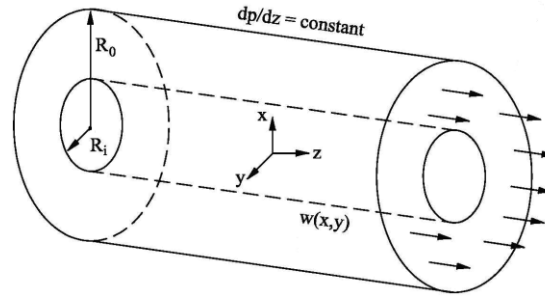

Figure 1. Schematic of the concentric annulus and co-ordinate system.

In the system to be analysed, the z co-ordinate represents the axial direction and the x–y co-ordinate plane is attached to the cross-sectional surface. To simplify the problem and its solution, the steady laminar flow is assumed to be fully developed with constant transport properties and negligible body forces. Under these conditions, the Navier-Stokes equation becomes the simple pressure-driven Poiseuille flow equation. Because the flow is fully developed, the axial flow velocity is a function of only the x and y co-ordinates, and the axial pressure gradient is constant. In the energy equation, the viscous dissipation and axial heat conduction are neglected.

2.1. Governing Equations

The governing equations of the laminar fluid flow, expressed in the form of a Poisson equation, are obtained from the momentum and energy conservation equations [49]:

$$\nabla^2 w = \frac{\partial^2 w}{\partial x^2} + \frac{\partial^2 w}{\partial y^2} = \frac{1}{\eta} \frac{dp}{dz} \tag{1}$$

$$\nabla^2 T = \frac{\partial^2 T}{\partial x^2} + \frac{\partial^2 T}{\partial y^2} = \frac{w}{a} \frac{dT}{dz} \tag{2}$$

where w is the axial velocity of the flow; η is the dynamic viscosity; p is the pressure; T is the temperature; and $a = \lambda/\rho c$ is the thermal diffusivity.

For the fully developed thermal flow with constant heat flux on the boundaries and using the mixed mean temperature T_m [48], Equation (2) becomes:

$$\nabla^2 T = \frac{\partial^2 T}{\partial x^2} + \frac{\partial^2 T}{\partial y^2} = \frac{w}{a} \frac{dT_m}{dz} \tag{3}$$

where $\partial T/\partial z = dT_m/dz$ is a constant derived from the given conditions.

2.2. Boundary Conditions

The boundary conditions associated with Equations (1) and (3) are:

$$w = 0 \text{ at } r = R_i \text{ and } r = R_o \tag{4}$$

$$T = T_i \text{ at } r = R_i; \quad T = T_o \text{ at } r = R_o \tag{5}$$

where R_i is the radius of the inner cylinder and R_o is the radius of the outer cylinder.

To solve for the temperature, the velocity is first obtained from Equation (1); then Equation (3) can be solved, because the assumption of negligible buoyancy decouples the momentum and energy equations.

3. Numerical Model

3.1. The DRM Formulation

To solve using the BEM, Equations (1) and (3) subject to Equations (4) and (5) can be generalized as the following type of Poisson equation [43]:

$$\nabla^2 u(x,y) = b(x,y), \qquad (x,y) \in \Omega \tag{6}$$

with the boundary conditions:

$$u(x,y) = \overline{u}, \qquad (x,y) \in \Gamma_1 \tag{7}$$

$$q(x,y) = \frac{\partial u(x,y)}{\partial n} = \overline{q}, \quad (x,y) \in \Gamma_2 \tag{8}$$

and the convective heat transfer problem is represented by:

$$\begin{aligned} u(x,y) = w, & \quad b(x,y) = \frac{1}{\eta}\frac{\mathrm{d}p}{\mathrm{d}z} = \text{const.} \\ u(x,y) = T, & \quad b(x,y) = \frac{w}{a}\frac{\mathrm{d}T_m}{\mathrm{d}z} \end{aligned} \tag{9}$$

where: $\Gamma_1 + \Gamma_2 = \Gamma$ is the total boundary of the domain Ω; n is normal to the boundary; and $\overline{u}$ and $\overline{q}$ are the values specified at each boundary.

Applying the usual boundary element technique to Equation (6), an integral Equation can be derived as described in [21]:

$$c_i u_i + \int_\Gamma u q^* \mathrm{d}\Gamma - \int_\Gamma q u^* \mathrm{d}\Gamma = \int_\Omega b u^* \mathrm{d}\Omega \tag{10}$$

where the constant c_i depends on the geometry at point i as follows:

$$c_i = \begin{cases} 1 & \text{for } (x_i, y_i) \in \Omega \\ \frac{\theta}{2\pi} & \text{for } (x_i, y_i) \in \Gamma \end{cases} \tag{11}$$

where θ is the internal angle at the source point.

The key part of the DRM is to calculate the domain integral term of Equation (10) on the boundary and remove the need for a complicated domain discretization. To accomplish this, the source term $b(x, y)$ is expanded, using its values at each node j and a set of interpolating functions f_j as in [41,42]:

$$b(x,y) \cong \sum_{j=1}^{N+L} \alpha_j f_j \tag{12}$$

where α_j is a set of initially unknown coefficients; and N and L are the number of boundary nodes and internal points, respectively.

Using Equation (12), the coefficients α_j can be expressed in terms of the nodal values of the function $b(x, y)$ in matrix form as:

$$\boldsymbol{\alpha} = \mathbf{F}^{-1}\mathbf{b} \tag{13}$$

where $\mathbf{F}$ is a matrix with coefficients f_j and $\mathbf{b} = \{b_i\}$.

The radial basis functions f_j are linked with the particular solutions $\hat{u}_j$ to the equation:

$$\nabla^2 \hat{u}_j = f_j \tag{14}$$

Substituting Equation (14) into Equation (12) and applying integration by parts to the domain integral term of Equation (10) twice leads to:

$$c_i u_i + \int_\Gamma u q^* d\Gamma - \int_\Gamma q u^* d\Gamma = \sum_{j=1}^{N+L} \alpha_j \left(c_i \hat{u}_{ij} + \int_\Gamma \hat{u}_j q^* d\Gamma - \int_\Gamma \hat{q}_j u^* d\Gamma \right) \tag{15}$$

On a two-dimensional domain, u^*, q^* and $\hat{u}$, $\hat{q}$ can be derived as:

$$u^* = \frac{1}{2\pi} \ln\left(\frac{1}{r}\right); \quad q^* = \frac{-1}{2\pi r} \nabla r \cdot \vec{n} \tag{16}$$

$$\hat{u} = \frac{r^2}{4} + \frac{r^3}{9}; \quad \hat{q} = \left(\frac{r}{2} + \frac{r^2}{3}\right) \nabla r \cdot \vec{n} \tag{17}$$

where r is the distance from a source point i, or a DRM collocation point j to a field point (x, y). As for Equation (14), an interpolating function is chosen as a radial basis function (RBF). Two relevant expressions for RBFs are frequently used for this purpose in the engineering community: $f = 1 + r$ and $f = 1 + r + r^2$ [44,45].

In the numerical solution of the integral Equation (15), u, q, $\hat{u}$ and $\hat{q}$ are modelled using the linear interpolation functions as follows:

$$\int_{\Gamma_k} u q^* d\Gamma = u_k h_{ik}^1 + u_{k+1} h_{ik}^2 \tag{18}$$

$$\int_{\Gamma_k} q u^* d\Gamma = q_k g_{ik}^1 + q_{k+1} g_{ik}^2 \tag{19}$$

$$\int_{\Gamma_k} \hat{u}_j q^* d\Gamma = \hat{u}_{kj} h_{ik}^1 + \hat{u}_{(k+1)j} h_{ik}^2 \tag{20}$$

$$\int_\Gamma \hat{q}_j u^* d\Gamma = \hat{q}_{kj} g_{ik}^1 + \hat{q}_{(k+1)j} g_{ik}^2 \tag{21}$$

where:

$$h_{ik}^1 = \int_{\Gamma_k} \Phi_1 q^* d\Gamma, \quad h_{ik}^2 = \int_{\Gamma_k} \Phi_2 q^* d\Gamma \tag{22}$$

$$g_{ik}^1 = \int_{\Gamma_k} \Phi_1 u^* d\Gamma, \quad g_{ik}^2 = \int_{\Gamma_k} \Phi_2 u^* d\Gamma \tag{23}$$

The first subscript in Equations (22) and (23) refers to the specific position of the point where the flow velocity or temperature is evaluated. The second subscript refers to the boundary element over which the contour integration is performed. The superscripts 1 and 2 designate the linear interpolation functions Φ_1 and Φ_2, respectively, with which the u^* and q^* functions are weighted in the integrals in Equations (18) to (21).

When the boundary $\Gamma = \Gamma_1 \cup \Gamma_2$ is discretized into N elements, the integral terms in Equation (15) can be rewritten as:

$$\int_\Gamma u q^* d\Gamma = \sum_{k=1}^N \int_{\Gamma_k} u q^* d\Gamma = \sum_{k=1}^N \left[h_{i(k-1)}^2 + h_{ik}^1 \right] u_k = \sum_{k=1}^N H_{ik} u_k \text{ or } = \sum_{j=1}^{N_n} H_{ik} \hat{u}_{kj} \quad \text{for } \hat{u}_j \tag{24}$$

$$\int_\Gamma q u^* d\Gamma = \sum_{k=1}^N \int_{\Gamma_k} q u^* d\Gamma = \sum_{k=1}^N \left[g_{i(k-1)}^2 + g_{ik}^1 \right] q_k = \sum_{k=1}^N G_{ik} q_k \text{ or } = \sum_{j=1}^{N_n} G_{ik} \hat{q}_{kj} \quad \text{for } \hat{q}_j \tag{25}$$

where $h_{i0}^2 = h_{iN}^2$ and $g_{i0}^2 = g_{iN}^2$.

Substituting Equations (24) and (25) into Equation (15), after several manipulations, yields the dual reciprocity boundary element Equation:

$$c_i u_i + \sum_{k=1}^{N} H_{ik} u_k - \sum_{k=1}^{N} G_{ik} q_k = \sum_{j=1}^{N+L} \alpha_j \left(c_i \hat{u}_{ij} + \sum_{k=1}^{N} H_{ik} \hat{u}_{kj} - \sum_{k=1}^{N} G_{ik} \hat{q}_{kj} \right) \tag{26}$$

3.2. Numerical Solution

Equation (26) can now be written in a matrix-vector form as:

$$\mathbf{HU} - \mathbf{GQ} = (\mathbf{H\hat{U}} - \mathbf{G\hat{Q}})\boldsymbol{\alpha} \tag{27}$$

where $\mathbf{H}$ and $\mathbf{G}$ are matrices with elements H_{ik} and G_{ik}, with c_i incorporated into the principal diagonal element; and $\mathbf{U}$, $\mathbf{Q}$ and their terms $\mathbf{\hat{U}}$, $\mathbf{\hat{Q}}$ correspond to vectors with elements u_k and q_k, and matrices with $\hat{u}_{kj}$ and $\hat{q}_{kj}$ as the jth column vectors.

Substituting $\boldsymbol{\alpha}$ from Equation (13) into the above equation yields:

$$\mathbf{HU} - \mathbf{GQ} = (\mathbf{H\hat{U}} - \mathbf{G\hat{Q}})\mathbf{F}^{-1}\mathbf{b} \tag{28}$$

Introducing the boundary conditions into the nodes of the u_k and q_k vectors, and rearranging by moving known quantities to the right-hand side and unknown quantities to the left-hand side, leads to a system of linear equations of the form:

$$\mathbf{AX} = \mathbf{B} \tag{29}$$

Using the DRM matrix equation, a numerical solution to the problem of laminar convective heat transfer between two concentric cylinders can be readily obtained for the flow velocity w from the momentum equation, and the temperature T from the energy equation or for their normal derivatives.

This numerical model has been implemented as a computer program in the FORTRAN programming language for PC-compatible microsystems.

3.3. Testing the Model

The geometry illustrated in Figure 2 is used for testing purposes. To simplify the problem, the surface temperatures of the two cylinders are assumed to be equal. Thus, the solution satisfies the following boundary conditions:

$$\begin{aligned}
w(x,y)|_{R=R_i} &= w(x,y)|_{R=R_o} = 0 \\
T*(x,y)|_{R=R_i} &= T*(x,y)|_{R=R_o} = 0 \\
T* &= T - T_w, \quad T_w = T_i = T_o
\end{aligned} \tag{30}$$

For the numerical test case, the following numerical values are introduced to Equations (1) and (3) from [50], in which the spectral collocation method is used to analyse heat convection in an eccentric annulus:

$$\begin{aligned}
R_i &= 0.030\,\text{m}, \quad R_o = 0.055\,\text{m} \\
\tfrac{1}{\eta}\tfrac{dp}{dz} &= -836\,\text{m}^{-1}\text{s}^{-1} \\
a &= 1.3418 \times 10^{-9}\,\text{m}^2/\text{s} \\
\tfrac{dT_m}{dz} &= 0.47\,°\text{C/m}
\end{aligned} \tag{31}$$

To confirm the accuracy of the DRM for the actual heat convection problem, the boundaries of the external and internal surfaces are discretized into 36, 48, 60, 72, or 84 elements. The nodes on every boundary and at the internal points of the analysis domain are located as shown in Figure 2. Therefore, the total number of internal points used in the analysis is 90, 120, 150, 180, and 210 in the 36, 48, 60, 72, and 84 boundary element cases, respectively.

Some statistical methods, such as the root mean square error (RMSE), the coefficient of variation (c_v), the coefficient of multiple determinations (R^2), and the relative error (e_r) may be used to compare simulated and analytical (exact) values of the flow's velocity and temperature to validate the model.
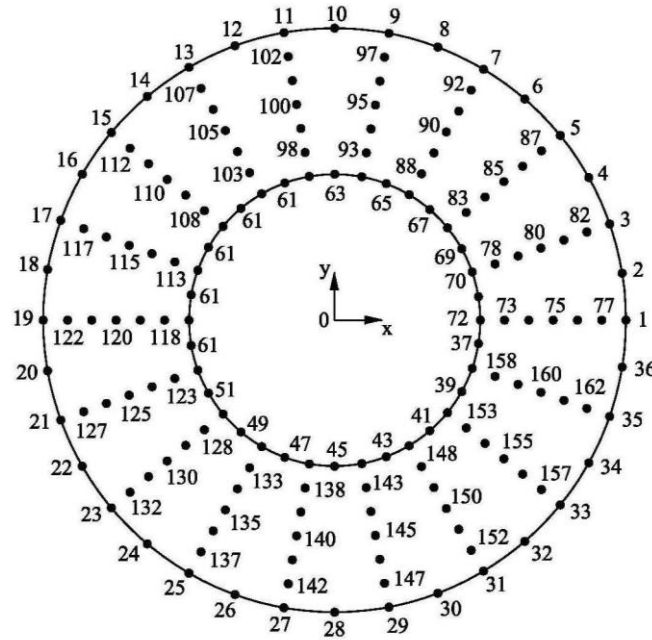

Figure 2. Boundary element nodes and internal points.

The error can be estimated using the RMSE, defined as [51]:

$$\text{RMSE} = \sqrt{\frac{\sum_{i=1}^{n} \left(y_{\text{sim},i} - y_{\text{anal},i}\right)^2}{n}} \tag{32}$$

In addition, the coefficient of variation c_v, in percent, and the coefficient of multiple determinations R^2 are defined as follows:

$$c_v = \frac{\text{RMSE}}{\left|\overline{y}_{\text{anal},i}\right|} 100\% \tag{33}$$

$$R^2 = 1 - \frac{\sum_{i=1}^{n} \left(y_{\text{sim},i} - y_{\text{anal},i}\right)^2}{\sum_{i=1}^{n} y_{\text{anal},i}^2} \tag{34}$$

where n is the number of analytical data points in the independent data set; $y_{\text{anal},i}$ is the analytical value of one data point i; $y_{\text{sim},i}$ represents the simulated value; and $\overline{y}_{\text{anal},i}$ is the mean value of all of the analytical data points.

The relative error e_r is calculated using the following formula:

$$e_r = \frac{\left|y_{\text{anal},i} - y_{\text{sim},i}\right|}{y_{\text{sim},i}} 100\% \tag{35}$$

where $y_{\text{anal},i}$ is the analytical solution; and $y_{\text{sim},i}$ is the potential value at point i obtained by the numerical method.

4. Simulation Results and Discussion

To obtain the axial flow velocity w (x, y), Equation (1) is solved first. The results for the boundary and internal nodes are shown in Tables 1 and 2 for the RBFs $f = 1 + r$ and $f = 1 + r + r^2$, respectively. In these tables, the normal derivative of the velocity w at the boundary is also listed, and all of the numerical solutions are compared with the exact solutions [47], in order to determine their accuracy. In addition, statistical values such as the RMSE, c_v, and R^2, which correspond to different numbers of boundary elements in the analysed system, are given in Tables 1 and 2.

Table 1. Dual reciprocity method (DRM) results and analytical solution for the boundary and internal points in flow velocity simulation ($f = 1 + r$).

Variable	Radial Location r [m]	DRM Solution					Analytical Solution
		Number of Boundary Elements					
		36	48	60	72	84	
$\partial w/\partial n$	0.055	−9.570611	−9.614363	−9.632446	−9.646733	−9.649446	−9.667904
$\partial w/\partial n$	0.030	−11.961390	−11.931682	−11.910987	−11.902295	−11.900702	−11.883840
w	0.0342	0.040336	0.039937	0.039755	0.039656	0.039614	0.039413
w	0.0383	0.061518	0.061112	0.060926	0.060825	0.060760	0.060591
w	0.0425	0.066727	0.066320	0.066133	0.066030	0.065973	0.065803
w	0.0466	0.057611	0.057196	0.057006	0.056908	0.056853	0.056682
w	0.0508	0.035084	0.034883	0.034733	0.034638	0.034606	0.034439
	RMSE	0.000741	0.000427	0.000275	0.000191	0.000149	—
	c_v%	2.018	1.162	0.749	0.521	0.405	—
	R^2	0.999724	0.999908	0.999962	0.999981	0.999988	—

Table 2. DRM results and analytical solution for the boundary and internal points in flow velocity simulation ($f = 1 + r + r^2$).

Variable	Radial Location r [m]	DRM Solution					Analytical Solution
		Number of Boundary Elements					
		36	48	60	72	84	
$\partial w/\partial n$	0.055	−9.570477	−9.615427	−9.632632	−9.647164	−9.651780	−9.667904
$\partial w/\partial n$	0.030	−11.960900	−11.929878	−11.906732	−11.899952	−11.898130	−11.883840
w	0.0342	0.040334	0.039938	0.039754	0.039654	0.039601	0.039413
w	0.0383	0.061519	0.061112	0.060927	0.060820	0.060761	0.060591
w	0.0425	0.066725	0.066321	0.066136	0.066031	0.065974	0.065803
w	0.0466	0.057609	0.057193	0.057012	0.056906	0.056850	0.056682
w	0.0508	0.035080	0.034880	0.034726	0.034635	0.034604	0.034439
	RMSE	0.000740	0.000426	0.000276	0.000189	0.000146	—
	c_v%	2.015	1.160	0.750	0.516	0.397	—
	R^2	0.999725	0.9999087	0.999961	0.999982	0.999989	—

Figures 3 and 4 shows the convergence of the DRM's solutions for the velocity and its normal derivative, as the numbers of boundary elements and internal points increase. The DRM solutions agree well with the exact solutions, and the relative errors are within 2.3% when the number of elements is greater than 36. The values of the RMSE and c_v are between 0.00014% and 0.00074%, and 0.40% and 2.01%, respectively, for the two radial basis functions. The R^2-value for any number of boundary elements is approximately 0.9997% for both of the radial basis functions, a result that is very satisfactory. Thus, the simulation model is analytically validated.
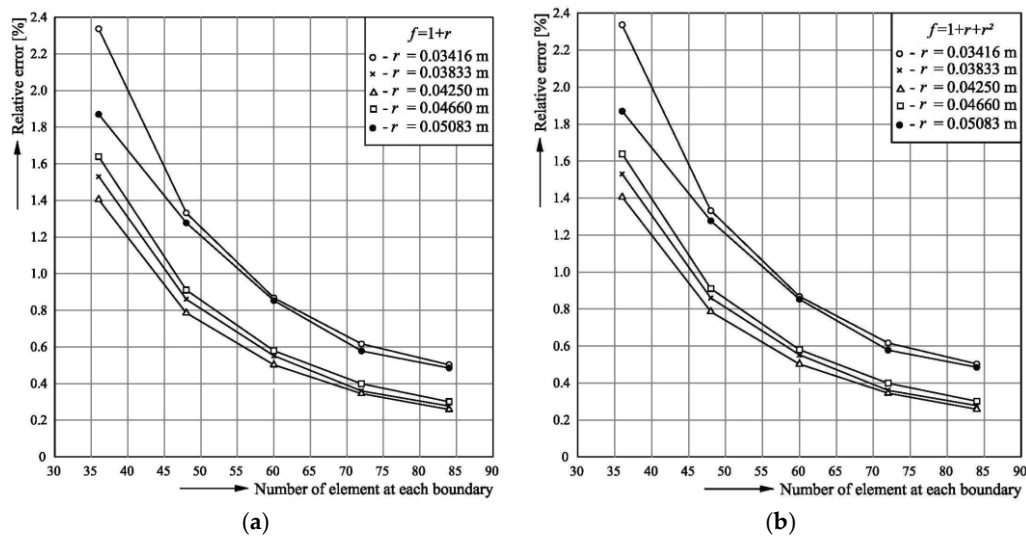
Figure 3. Accuracy of the solution for the velocity at the internal points: (**a**) Radial basis function $f = 1 + r$; (**b**) Radial basis function $f = 1 + r + r^2$.
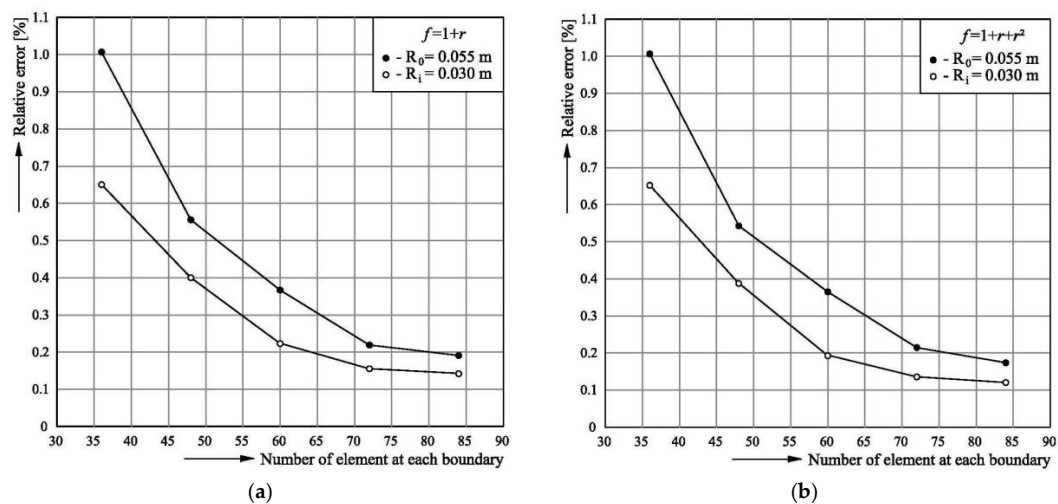

Figure 4. Magnitude of the error in the solution for the normal derivative of the velocity at the boundaries: (**a**) Radial basis function $f = 1 + r$; (**b**) Radial basis function $f = 1 + r + r^2$.

As noted in Figure 3, the velocities calculated at $r = 0.0508$ m and $r = 0.0342$ m are less accurate than the others, and the solution at $r = 0.0342$ is less accurate than it is at $r = 0.0508$. The solutions for the normal derivative of the velocity on the boundary at $r = 0.055$ m is less accurate than it is at $r = 0.030$ m, as shown in Figure 4. This is because the outer boundary elements are larger than the inner boundary elements, and the distribution of internal points becomes sparse in the outward direction, whereas a rapid change in the velocity occurs at the inner and outer boundaries, as shown in Figures 2 and 5.
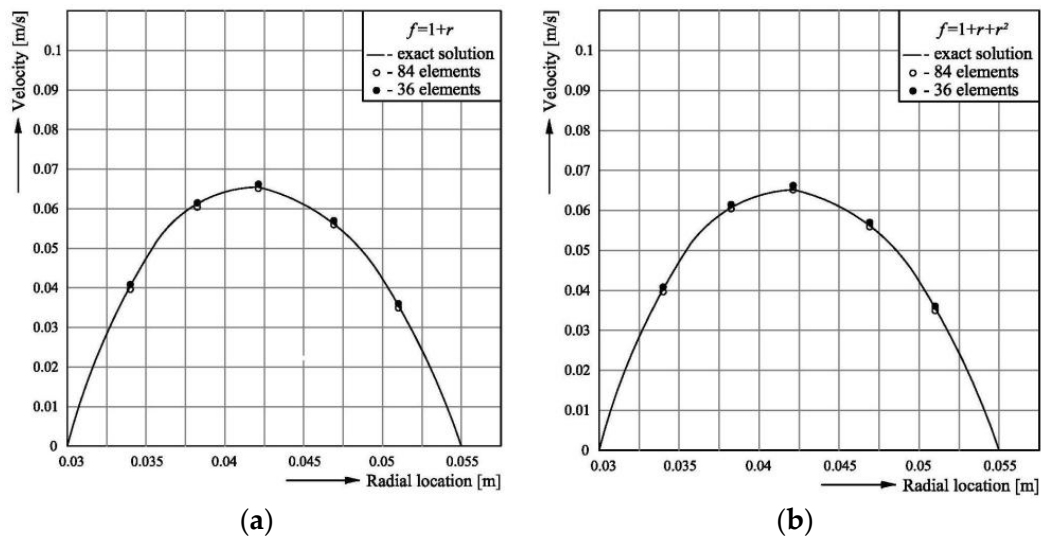
Figure 5. Comparison of velocity profile obtained using analytical solution and DRM results: (**a**) Radial basis function $f = 1 + r$; (**b**) Radial basis function $f = 1 + r + r^2$.

Therefore, the magnitude of the solution's error in the radial direction is closely related to the physical and the mathematical aspects of the problem; hence, the overall accuracy of the solution is fairly acceptable. Therefore, when 36 elements are used, the solution has a maximum error of 2.34% at radial position $r = 0.0342$ m, and the next step results in an accurate solution for the temperature. The DRM solutions for the velocity are, in turn, used in the energy equation (Equation (3)) to solve for the temperature distribution. Tables 3 and 4 show the simulation results for temperature and statistical values such as the RMSE, c_v, and R^2. The DRM solutions are in excellent agreement with the exact solutions and the relative errors e_r are within 5% when 36 elements are used (Figures 6–8). The c_v values are in the range of 0.3%–5.0%, and the R^2-value is approximately 0.999 for the two radial basis functions with any of the tested numbers of boundary elements. This is a very acceptable result, and thus, the simulation model is validated by the analytical solutions.

Table 3. DRM results and analytical solution for boundary and internal points in temperature ($f = 1 + r$).

Variable	Radial Location r [m]	DRM Solution					Analytical Solution
		Number of Boundary Elements					
		36	48	60	72	84	
$\partial T^*/\partial n$	0.055	172056.38	170824.22	171362.75	171600.75	171628.56	170484.20
$\partial T^*/\partial n$	0.030	233420.45	229217.02	230340.65	230698.70	230771.22	229506.90
T^*	0.0342	804.26	828.59	847.40	853.78	855.04	858.72
T^*	0.0383	1268.86	1298.52	1311.65	1315.86	1317.26	1320.13
T^*	0.0425	1383.48	1413.28	1426.46	1429.68	1431.26	1433.69
T^*	0.0466	1180.68	1209.26	1224.48	1230.46	1231.92	1234.96
T^*	0.0508	711.52	730.65	741.78	746.86	747.90	750.34
RMSE		42.3739	20.1408	7.8869	3.6070	2.4750	—
$c_v\%$		5.298	2.518	0.986	0.451	0.309	—
R^2		0.998102	0.999571	0.99934	0.999986	0.999993	—

Table 4. DRM results and analytical solution for the boundary and internal points in temperature ($f = 1 + r + r^2$).

Variable	Radial Location r [m]	DRM Solution					Analytical Solution
		Number of Boundary Elements					
		36	48	60	72	84	
$\partial T^*/\partial n$	0.055	171989.88	170768.08	171293.14	171535.45	171598.75	170484.20
$\partial T^*/\partial n$	0.030	233300.36	229286.02	230294.05	230618.22	230708.55	229506.90
T^*	0.0342	805.85	829.69	848.14	854.14	855.78	858.72
T^*	0.0383	1271.14	1299.86	1312.24	1316.04	1317.68	1320.13
T^*	0.0425	1385.24	1414.58	1427.24	1430.02	1431.76	1433.69
T^*	0.0466	1182.72	1210.64	1225.78	1230.98	1232.04	1234.96
T^*	0.0508	713.38	731.68	742.87	747.12	748.03	750.34
	RMSE	40.7741	19.1179	7.1300	3.3248	2.1458	—
	$c_v\%$	5.098	2.390	0.891	0.415	0.268	—
	R^2	0.998243	0.999613	0.999946	0.999988	0.999995	—

(a)　　　　　　　　　　　　　　　　(b)
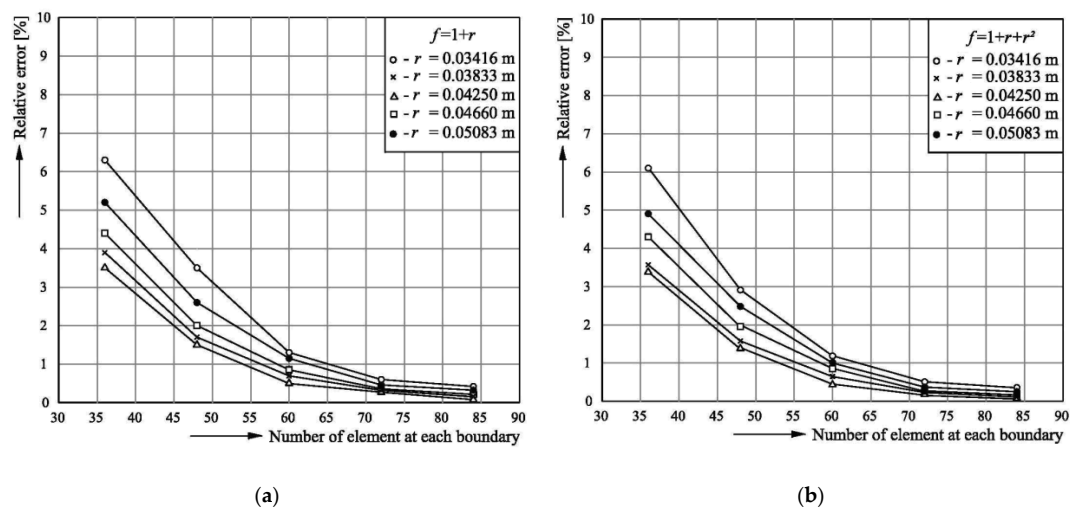
Figure 6. Accuracy of the solution for the temperature at the internal points: (**a**) Radial basis function $f = 1 + r$; (**b**) Radial basis function $f = 1 + r + r^2$.

(a)　　　　　　　　　　　　　　　　(b)
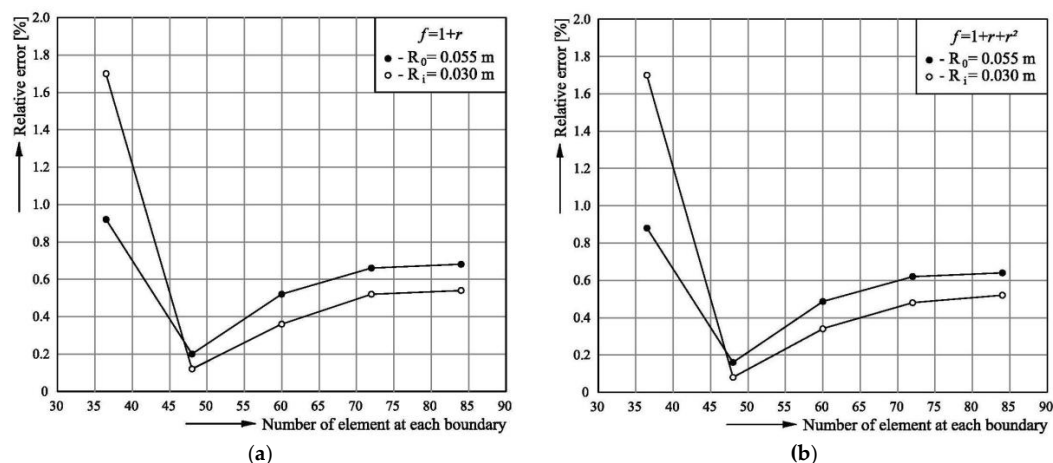
Figure 7. Accuracy of the solution for the normal derivative of the temperature at the boundaries: (**a**) Radial basis function $f = 1 + r$; (**b**) Radial basis function $f = 1 + r + r^2$.
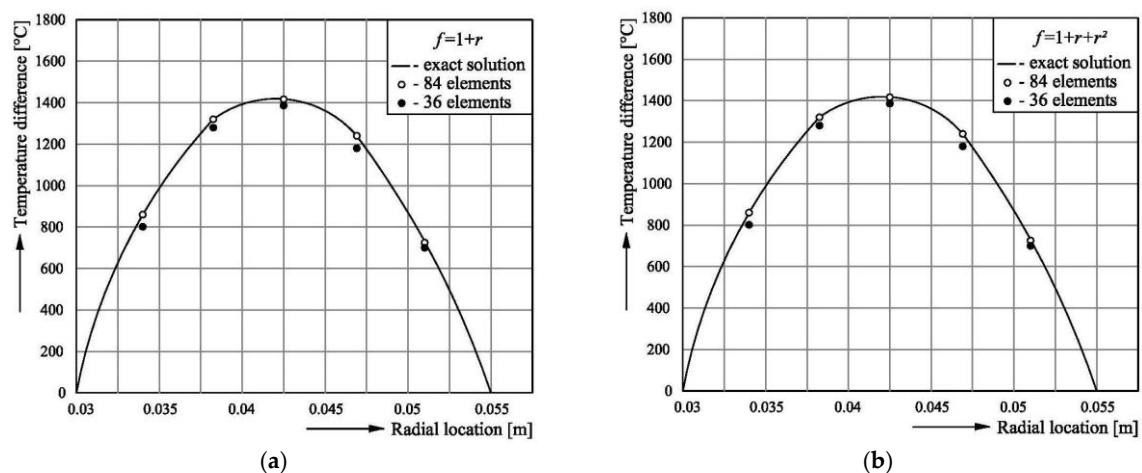
Figure 8. Comparison of temperature profile T^* obtained using analytical solution and DRM results: (**a**) Radial basis function $f = 1 + r$; (**b**) Radial basis function $f = 1 + r + r^2$.

Although the convergence trend shown in Figure 7 is not monotonic and the radial location's effect on the magnitude of the error does not exactly follow the trend shown in the previous case, the solution trends can be considered indistinguishable within 1% relative error.

These test results validate the power of the dual reciprocity boundary element method and the accuracy of its solutions. This is because the numerical solution for the velocity was used as an input in Equation (3), and the source-like function $b(x, y)$ of Equation (12) in Equation (3) was approximated using interpolating functions and the nodal values of internal points.

As a final note, all of the numbers of elements tested are adequate for solving this problem. The amount of error in the solutions for the velocity and temperature is acceptable. Using the fourth-order RBFs, the accuracy of the DRM is increased insignificantly, so that only minor differences are observed between errors (0.2%). The errors can be decreased using only a higher adequate number of boundary elements and internal points limited by computational capacity.

5. Conclusions

A numerical simulation model based on the dual reciprocity boundary element method has been developed for the solution of the laminar heat convection problem between two concentric cylinders with a constant imposed heat flux.

The DRM is different than the standard implementation, as was proposed for Poisson-type equations due the use of RBFs. The DRM matrix was formulated to perform numerical computation, and five boundary element discretizations were tested with corresponding numbers of internal points. Five radial locations were selected, at which solution for the velocity and temperature was obtained. The numerical results were shown to be in excellent agreement with exact solutions for the 36-element case, and the simulation model was analytically validated.

This numerical model was successfully used to solve the laminar convective heat transfer problem in a concentric annular tube. This study also shows that the DRM has strong potential for further applications. Although this method has been applied to 2D problems, an extension of the approach to 3D problems is straightforward.

Author Contributions: All authors conceived the research idea and the framework of this study. Iosif Anton performed the theoretical study and Ioan Sarbu analysed the data and wrote the paper. Both authors have read and approved the final manuscript.

References

1. Irons, B.M.; Ahmad, S. *Techniques of Finite Elements*; John Wiley: New York, NY, USA, 1980.
2. Rao, S. *The Finite Element Method in Engineering*; Pergamon Press: New York, NY, USA, 1981.
3. Nowak, A.J.; Brebbia, A.C. The multiple reciprocity method: A new approach for transforming BEM domain integrals to the boundary. *Eng. Anal.* **1989**, *6*, 164–167. [CrossRef]
4. Partridge, W.P.; Brebbia, A.C. Computer implementation of the BEM dual reciprocity method for the solution of general field Equations. *Commun. Appl. Numer. Methods* **1990**, *6*, 83–92. [CrossRef]
5. Chen, G.; Zhou, J. *Boundary Element Methods*; Academic Press: New York, NY, USA, 1992.
6. Reddy, J.N. *An Introduction to the Finite Element Method*; McGraw-Hill: New York, NY, USA, 1993.
7. Paris, F.; Cañas, J. *Boundary Element Method: Fundamentals and Applications*; Oxford University Press: Oxford, UK, 1997.
8. Power, H.; Mingo, R. The DRM Subdomain decomposition approach to solve the two-dimensional Navier-Stokes system of equations. *Eng. Anal. Bound. Elements* **2000**, *24*, 107–119. [CrossRef]
9. Sarbu, I. *Numerical Modelling and Optimizations in Building Services*; Polytechnic Publishing House: Timisoara, Romania, 2010. (In Romanian)
10. Lavine, A.S.; Incropera, F.P.; Dewitt, D.P. *Fundamentals of Heat and Mass Transfer*; John Wiley & Sons: New York, NY, USA, 2011.
11. Popov, V.; Bui, T.T. A meshless solution to two-dimensional convection-diffusion problems. *Eng. Anal. Bound. Elements* **2010**, *34*, 680–689. [CrossRef]
12. Bai, F.; Lu, W.Q. The selection and assemblage of approximating functions and disposal of its singularity in axisymmetric DRBEM for heat transfer problems. *Eng. Anal. Bound. Elements* **2004**, *28*, 955–965. [CrossRef]
13. Asad, A.S. Heat transfer on axis symmetric stagnation flow an infinite circular cylinder. In Proceedings of the 5th WSEAS International Conference on Heat and Mass Transfer, Acapulco, Mexico, 25–27 January 2008; pp. 74–79.
14. Nekoubin, N.; Nobari, M.R.H. Numerical analysis of forced convection in the entrance region of an eccentric curved annulus. *Numer. Heat Transf. Appl.* **2014**, *65*, 482–507. [CrossRef]
15. Wang, B.L.; Tian, Y.H. Application of finite element: Finite difference method to the determination of transient temperature field in functionally graded materials. *Finite Elements Anal. Des.* **2005**, *41*, 335–349. [CrossRef]
16. Wu, Q.; Sheng, A. A Note on finite difference method to analysis an ill-posed problem. *Appl. Math. Comput.* **2006**, *182*, 1040–1047. [CrossRef]
17. Shakerim, F.; Dehghan, M. A finite volume spectral element method for solving magnetohydrodynamic (MHD) equations. *Appl. Numer. Math.* **2011**, *61*, 1–23. [CrossRef]
18. Sammouda, H.; Belghith, A.; Surry, C. Finite element simulation of transient natural convection of low-Prandtl-number fluids in heated cavity. *Int. J. Numer. Methods Heat Fluid Flow* **1999**, *5*, 612–624. [CrossRef]
19. Sarbu, I. Numerical analysis of two-dimensional heat conductivity in steady state regime. *Period. Polytech. Mech. Eng.* **2005**, *49*, 149–162.
20. Wang, B.L.; Mai, Y.W. Transient one dimensional heat conduction problems solved by finite element. *Int. J. Mech. Sci.* **2005**, *47*, 303–317. [CrossRef]
21. Brebbia, C.A.; Telle, J.C.; Wrobel, I.C. *Boundary Element Techniques*; Springer-Verlag: New York, NY, USA, 1984.
22. Kane, J.H. *Boundary Element Analysis in Engineering Continuum Mechanics*; Prentice–Hall: New Jersey, NJ, USA, 1994.
23. Goldberg, M.A.; Chen, C.S.; Bowman, H. Some recent results and proposals for the use of radial basis functions in the BEM. *Eng. Anal. Bound. Elements* **1999**, *23*, 285–296. [CrossRef]
24. Yang, K.; Peng, H.-F.; Cui, M.; Gao, X.-W. New analytical expressions in radial integration BEM for solving heat conduction problems with variable coefficients. *Eng. Anal. Bound. Elements* **2015**, *50*, 224–230. [CrossRef]
25. Sedaghatjoo, Z.; Adibi, H. Calculation of domain integrals of two dimensional boundary element method. *Eng. Anal. Bound. Elements* **2012**, *36*, 1917–1922. [CrossRef]
26. Divo, E.A.; Kassab, A.J. *Boundary Element Methods for Heat Conduction: Applications in Non-Homogeneous Media*; WIT Press: Southampton, NY, USA, 2003.
27. Žagar, I.; Škerget, L. Boundary elements for time dependent 3-D laminar viscous fluid flow. *J. Mech. Eng.* **1989**, *35*, 160–163.

28. Choi, C.Y. Detection of cavities by inverse heat conduction boundary element method using minimal energy technique. *J. Korean Soc. Non-Destr. Test.* **1997**, *17*, 237–247.

29. Garimella, S.; Dowling, W.I.; van der Veen, M.; Killion, J. Heat transfer coefficients for simultaneously developing flow in rectangular tubes. In Proceedings of the ASME 2000 International Mechanical Engineering Congress and Exposition, Orlando, FL, USA, 5–10 November 2000; 2, pp. 3–11.

30. Skerget, L.; Rek, Z. Boundary-domain integral method using a velocity-vorticity formulation. *Eng. Anal. Bound. Elements* **1995**, *15*, 359–370. [CrossRef]

31. Žunič, Z.; Hriberšek, M.; Škerget, L.; Ravnik, J. 3-D boundary element–finite element method for velocity–vorticity formulation of the Navier-Stokes equations. *Eng. Anal. Bound. Elements* **2007**, *31*, 259–266. [CrossRef]

32. Young, D.L.; Huang, J.L.; Eldho, T.I. Simulation of laminar vortex shedding flow past cylinders using a coupled BEM and FEM model. *Comput. Methods Appl. Mech. Eng.* **2001**, *190*, 5975–5998. [CrossRef]

33. Young, D.L.; Liu, Y.H.; Eldho, T.I. A combined BEM–FEM model for the velocity-vorticity formulation of the Navier-Stokes equations in three dimensions. *Eng. Anal. Bound. Elements* **2000**, *24*, 307–316. [CrossRef]

34. Ravnik, J.; Škerget, L.; Hriberšek, M. Two-dimensional velocity-vorticity based LES for the solution of natural convection in a differentially heated enclosure by wavelet transform based BEM and FEM. *Eng. Anal. Bound. Elements* **2006**, *30*, 671–686. [CrossRef]

35. Hsieh, K.J.; Lien, F.S. Numerical modeling of buoyancy-driven turbulent flows in enclosures. *Int. J. Heat Fluid Flow* **2004**, *25*, 659–670. [CrossRef]

36. Gao, X.W. The radial integration method for evaluation of domain integrals with boundary-only discretization. *Eng. Anal. Bound. Elements* **2002**, *26*, 905–916. [CrossRef]

37. Cui, M.; Gao, X.W.; Zhang, J.B. A new approach for the estimation of temperature-dependent thermal properties by solving transient inverse heat conduction problems. *Int. J. Therm. Sci.* **2012**, *58*, 113–119. [CrossRef]

38. Gao, X.W.; Peng, H.F. A boundary-domain integral equation method for solving convective heat transfer problems. *Int. J. Heat Mass Transf.* **2013**, *63*, 183–190. [CrossRef]

39. Peng, H.F.; Yang, K.; Gao, X.W. Element nodal computation-based radial integration BEM for non-homogeneous problems. *Acta Mech. Sin.* **2013**, *29*, 429–436. [CrossRef]

40. Nardini, D.; Brebbia, C.A. A new approach for free vibration analysis using boundary elements. In *Boundary Element Methods in Engineering*; Computational Mechanics Publications: Southampton, NY, USA, 1982; pp. 312–326.

41. Wrobel, C.L.; DeFigueiredo, D.B. A dual reciprocity boundary element formulation for convection diffusion problems with variable velocity fields. *Eng. Anal. Bound. Elements* **1991**, *8*, 312–319. [CrossRef]

42. Partridge, P.W.; Brebbia, C.A.; Wrobel, L.C. *The Dual Reciprocity Boundary Element Method*; Computational Mechanics Publications: Southampton, NY, USA, 1992.

43. Tezer-Sezgin, M.; Bozkaya, C.; Türk, Ö. BEM and FEM based numerical simulations for biomagnetic fluid flow. *Eng. Anal. Bound. Elements* **2013**, *37*, 127–1135. [CrossRef]

44. Yamada, T.; Wrobel, L.C.; Power, H. On the convergence of the dual reciprocity boundary element method. *Eng. Anal. Bound. Elements* **1994**, *13*, 91–298. [CrossRef]

45. Karur, S.R.; Ramachandran, P.A. Radial basis function approximation in the dual reciprocity method. *Math. Comput. Model.* **1994**, *20*, 59–70. [CrossRef]

46. Ilati, M.; Dehghan, M. The use of radial basis function (RBFs) collocation and RBF-QR methods for solving the coupled nonlinear Sine-Gordon equations. *Eng. Anal. Bound. Elements* **2015**, *52*, 99–109. [CrossRef]

47. Kays, W.M.; Crawford, M.E. *Convective Heat and Mass Transfer*; McGraw-Hill: New York, NY, USA, 1993.

48. Kakac, S.; Yener, Y.; Pramuanjaroenkij, A. *Convective Heat Transfer*; CRC Press: New York, NY, USA, 2014.

49. Jawarneh, A.M.; Vatistas, G.H.; Ababneh, A. Analytical approximate solution for decaying laminar swirling flows within narrow annulus. *Jordan J. Mech. Ind. Eng.* **2008**, *2*, 101–109.

50. Sim, W.G.; Kim, J.M. Application of spectral collocation method to conduction and laminar forced heat convection in eccentric annuli. *KSME Int. J.* **1996**, *10*, 94–104. [CrossRef]

51. Bechthler, H.; Browne, M.W.; Bansal, P.K.; Kecman, V. New approach to dynamic modelling of vapour-compression liquid chillers: Artificial neural networks. *Appl. Therm. Eng.* **2001**, *21*, 941–953. [CrossRef]